Energetic Limits of Phosphotransfer in the Catalytic Subunit of cAMP-Dependent Protein Kinase As Measured by Viscosity Experiments†

Joseph A. Adams and Susan S. Taylor*

Department of Chemistry, University of California, San Diego, 9500 Gilman Drive, La Jolla, California 92093-0654

Received February 3, 1992; Revised Manuscript Received May 4, 1992

ABSTRACT: Viscosogenic agents were used to test the diffusion limits of the reaction catalyzed by the catalytic subunit of the cAMP-dependent protein kinase. The effects of glycerol and sucrose on the maximum rate (k_{cat}) and the apparent second-order rate constants ($k_{cat}/K_{peptide}$) for the phosphorylation of four peptidic substrates were measured at their pH optima. The agents were found to have moderate to no effect on $k_{cat}/K_{peptide}$ for good and poor substrates, respectively. Conversely, k_{cat} was highly sensitive to solvent viscosity for three of the four peptides at high concentrations of ATP. Taken together, these data indicate that enzymatic phosphorylation by the catalytic subunit proceeds with rapid or near rapid equilibrium binding of substrates and that all steps following the central substrate complex (i.e., chemical and conformational events) are fast relative to the rate-determining dissociation of product, ADP, when ATP levels are high. Under saturating concentrations of peptide I, LRRASLG, an unproductive form of the enzyme is populated. The observed phosphorylation rate from this complex is involved in rate limitation owing to a slow step separating unproductive and productive enzyme forms. The data are used to establish a kinetic mechanism for the catalytic subunit that predicts initial reaction velocities under varying concentrations of ATP and substrate.

Protein phosphorylation levels in the cell are linked to the regulation of metabolic pathways, cell division, and oncogenesis (Hanks et al., 1985; Cooper, 1990). The importance of protein kinases for the homeostasis of living cells has prompted a wide range of physical studies including chemical modification, cellular localization, mutagenesis, and kinetic methods (Taylor et al., 1990). cAMP-dependent protein kinase (cAPK)[1] was one of the first protein kinases discovered (Walsh et al., 1968) and remains a simple model for the study of other enzymes of its class. In the absence of the second messenger, cAMP, cAPK exists in an inactive tetramer composed of two catalytic subunits and a regulatory dimer. The binding of cAMP to the regulatory portion induces a conformational change that leads to the immediate breakdown of the tetramer into its constituent catalytic and regulatory subunits. The catalytic subunit can then bind and phosphorylate protein or peptide substrates in an ATP-dependent manner. Peptide studies demonstrated that the catalytic subunit will preferentially phosphorylate serine or threonine in the consensus sequence R-R-X-S/T-Y, where X is variable and Y is a hydrophobic amino acid (Kemp et al., 1977).

The recent overexpression of soluble amounts of the catalytic subunit of cAPK in *Escherichia coli* (Slice & Taylor, 1989; Yonemoto et al., 1991) and the X-ray crystallographic solution of a binary peptide complex (Knighton et al., 1991a,b) make detailed physical studies possible. The use of site-directed mutagenesis to understand better the phosphorylation reaction will be foremost in these studies. The findings that mutagenized protein kinases with altered activities may be linked to various disease states including cellular oncogenesis (Hunter & Cooper, 1986) make mutagenesis studies attractive. However, a necessary precursor for the evaluation of this technique is the establishment of a complete kinetic mechanism including estimates of the rates of chemical and conformational changes and substrate and product dissociation. We have studied the dependence of the steady-state kinetic parameters on solution viscosity in an effort to put numerical constraints on these processes. Using this technique we have been able to define a kinetic phosphorylation mechanism at varying concentrations of peptide and ATP that includes measurements of the energetic barriers for a number of microscopic steps along the catalytic pathway. The data are consistent with the available steady-state kinetic, equilibrium binding, and inhibitor studies for cAPK. The mechanism provides a solid framework for the evaluation of the effects on the kinetic properties of site-directed mutants of the catalytic subunit.

MATERIALS AND METHODS

Materials. Adenosine 5′-triphosphate (ATP), phosphoenolpyruvate, magnesium chloride, and nicotinamide adenine dinucleotide, reduced (NADH), were purchased from Sigma. Glycerol and sucrose were purchased from Fisher Scientific and Mallinckrodt, respectively. Tris(hydroxymethyl)aminomethane (Tris) was purchased from Sigma. Pyruvate kinase from rabbit muscle and lactate dehydrogenase from bovine heart were purchased from Sigma.

Peptides and Protein. All peptides were synthesized at the Peptide and Oligonucleotide Facility at the University of California, San Diego. Peptides were purified by reverse-phase preparative HPLC chromatography. The concentration of peptides were determined by turnover with the catalytic subunit under conditions of limiting peptide. The recombinant catalytic subunit was expressed and purified from *E. coli* according to previously published procedures (Yonemoto et al., 1991). The concentration of enzyme was measured by A_{280} ($A_{0.1\%}$ = 1.2).

Kinetic Assay. The enzymatic activity of the catalytic subunit was measured spectrophotometrically (Cook et al.,

† This work was supported by NIH Research Grant GM 19301-20 to S.S.T. and NIH Training Grant DK 07044-12 to J.A.A.

* Author to whom correspondence should be addressed.

[1] Abbreviations: ADP, adenosine 5′-diphosphate; ATP, adenosine 5′-triphosphate; cAMP, adenosine cyclic 3′,5′-monophosphate; cAPK, cAMP-dependent protein kinase; NADH, nicotinamide adenine dinucleotide, reduced; Tris, tris(hydroxymethyl)aminomethane.

0006-2960/92/0431-8516$03.00/0

Table I: Synthetic Peptide Substrates

peptide	sequence
I (kemptide)[a]	LRRASLG
II (chocktide)[b]	LRRWSLG
III	LRRNSI
IV	LARNSI

[a] Peptide I is named after Bruce Kemp (Kemp et al., 1975). [b] Peptide II is named after P. Boon Chock (Wright et al., 1981).

Table II: Steady-State Kinetic Parameters and Viscosity Effects for Peptides I–IV at Saturating ATP Concentrations[a]

peptide	k_{cat} (s^{-1})	$K_{peptide}$ (μM)	$k_{cat}/K_{peptide}$ (μM^{-1} s^{-1})	$(k_{cat})^{\eta}$ [b]	$(k_{cat}/K_{peptide})^{\eta}$ [b]
I[c]	21 ± 1.0	65 ± 11	0.30 ± 0.030	1.0 ± 0.07	0.13 ± 0.07
II	17 ± 0.6	30 ± 4.1	0.56 ± 0.050	0.94 ± 0.14	0.40 ± 0.08
III	19 ± 1.0	42 ± 2.3	0.45 ± 0.025	1.1 ± 0.14	0.45 ± 0.11
IV	>2		(1.5 ± 0.3) × 10^{-4}		0[d]

[a] [ATP] = 1 mM, [peptide] = 10–200 μM, 10 mM free Mg^{2+}, 100 mM Tris (pH 8). Glycerol and sucrose were used as viscosogens as described in Materials and Methods. [b] $(k_{cat})^{\eta}$ and $(k_{cat}/K_{peptide})^{\eta}$ are the slopes of the plots of k_{cat}°/k_{cat} and $(k_{cat}/K_{peptide})^{\circ}/(k_{cat}/K_{peptide})$ vs η^{rel}. [c] The $K_{peptide}$ for peptide I was found to decrease slightly at lower Tris concentrations without affecting k_{cat}. For example, at 10 and 50 mM Tris, $K_{peptide}$ = 28 ± 4.2 μM and 48 ± 5.2 μM, respectively. [d] The ratios of $k_{cat}/K_{peptide}$ in the absence and presence of viscosogen are 1.0 ± 0.1, 0.95 ± 0.10, and 1.0 ± 0.07 at η^{rel} = 1, 1.8, and 3.2, respectively.

1982). This assay couples the production of ADP with the oxidation of NADH by pyruvate kinase and lactate dehydrogenase. Typically, varying amounts of ATP, peptide, and catalytic subunit were mixed manually with 1 mM phosphoenolpyruvate, 0.3 mM NADH, 12 units of lactate dehydrogenase, and 4 units of pyruvate kinase. All reactions were done in 100 mM Tris, pH 8.0, in the presence or absence of glycerol or sucrose at 24.0 °C. All assays contained 10–11 mM $MgCl_2$.

Solution Viscosity Measurements. The relative viscosity (η^{rel}) of buffers containing glycerol or sucrose was measured relative to a 100 mM Tris buffer at pH 8.0, 24.0 °C, using an Ostwald viscometer (Shoemaker & Garland, 1962). Glycerol buffers ranging between 0 and 36% (w/w) were used to obtain relative viscosity values between 1 and 2.2. A 30% (w/w) sucrose solution was used to obtain a relative viscosity of 3.2. All measurements of viscosity were performed in triplicate. Glycerol and sucrose had no effect on the extinction coefficient of NADH.

Data Analysis. The values of V_{max} and K_m were determined from plots of initial velocity vs substrate concentration according to

$$v = V_{max}[S]/(K_m + [S]) \quad (1)$$

where v is the initial velocity, [S] is the concentration of the varied substrate, V_{max} is the maximal velocity, and K_m is the Michaelis constant. The maximal velocity was then converted to k_{cat} by dividing V_{max} by the total enzyme concentration.

RESULTS

Steady-State Kinetic Parameters. The steady-state kinetic parameters for the cAPK-catalyzed phosphorylation of peptides I–IV (Table I) are listed in Table II. These data were collected from initial velocity traces under conditions of saturating ATP (1 mM) and varied peptide concentrations (10–200 μM) using the coupled enzyme assay at pH 8.0. The catalytic subunit was preequilibrated with ATP before initiation of the reaction with peptide. The concentrations of free and total Mg^{2+} were 10 and 11 mM, respectively. The

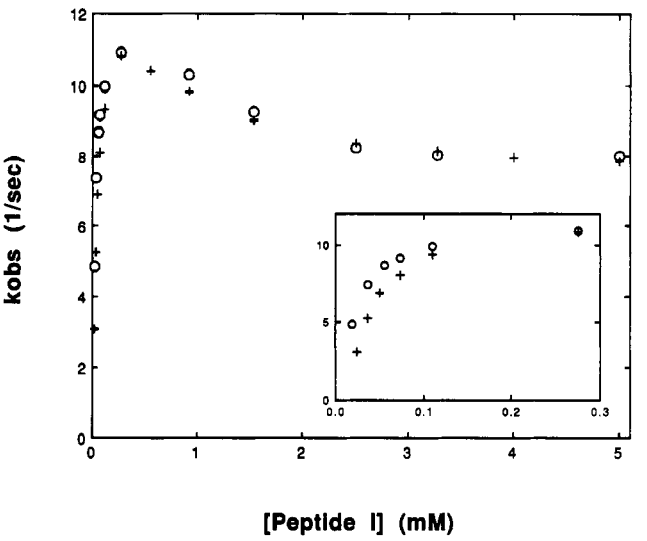

FIGURE 1: Dependence of the initial rate constant (k_{obs}) for the cAPK-catalyzed phosphorylation of peptide I at a fixed concentration of ATP (100 μM), 10 mM free Mg^{2+}, 24 °C, and 100 mM Tris (pH 8.0). The experimental data (O) were collected using 18–5000 μM peptide. The simulated data (+) were derived from the rate constants in Table IV and the mechanism in Scheme III using the kinetic simulation program HOPKINSIM.[3] A best approximation of the experimental data was achieved with k_{-2}/k_2 = 1000 $s^{-1}/2$ μM^{-1} s^{-1} = 500 μM (see Scheme III). The inset displays the experimental and simulated data for the hyperbolic portion of the plot (i.e., <0.3 mM).

maximum velocity for peptide IV could not be accurately determined owing to its weak affinity for the active site. A lower limit of 2 s^{-1} has been placed on k_{cat} for this peptide since this was the highest value attained in plots of velocity vs substrate concentration. The steady-state kinetic parameters for the phosphorylation of peptide I were also measured under conditions of varied peptide and 100 μM ATP at pH 8.0. Significant deviations from simple saturation kinetics occur at high concentrations of peptide I. This phenomenon is illustrated in the plot of Figure 1. At low peptide concentrations the data are hyperbolic (inset). At high concentrations, a plateau of approximately 8 s^{-1} is reached. The preequilibration of the catalytic subunit with either ATP or peptide I before initiation of the reaction had no effect on the observed initial velocity (data not shown).

Effects of Viscosogenic Agents on Enzyme Coupling Reagents. Since the rates of substrate phosphorylation were measured by coupling ADP production with NADH depletion in a coupled enzyme assay, it is important to ascertain the viability of the assay system under varying solution viscosities. Known concentrations of the catalytic subunit were mixed with ATP and peptide I in buffers containing either sucrose or glycerol. At relative viscosities (η^{rel}) of 1.8 (glycerol) and 3.2 (sucrose) the time-dependent production of ADP was proportional to the amount of catalytic subunit. At η^{rel} = 1.8, 110, 176, and 220 nM catalytic subunit produced 0.190, 0.301, and 0.376 μM ADP/s using 44 μM peptide I and 1 mM ATP. At η^{rel} = 3.2, 110 and 220 nM catalytic subunit produced 0.087 and 0.180 μM ADP/s using 88 μM peptide I and 1 mM ATP. Since the coupling reagents produced linear rate behavior, all further initial velocity data were collected at rates less than 0.40 μM ADP/s by the appropriate adjustment of enzyme concentration.

Effects of Viscosogenic Agents on Steady-State Kinetic Parameters. The steady-state kinetic parameters for the cAPK-catalyzed phosphorylation of peptides I–IV were measured in buffers of varying relative viscosity at pH 8.0.

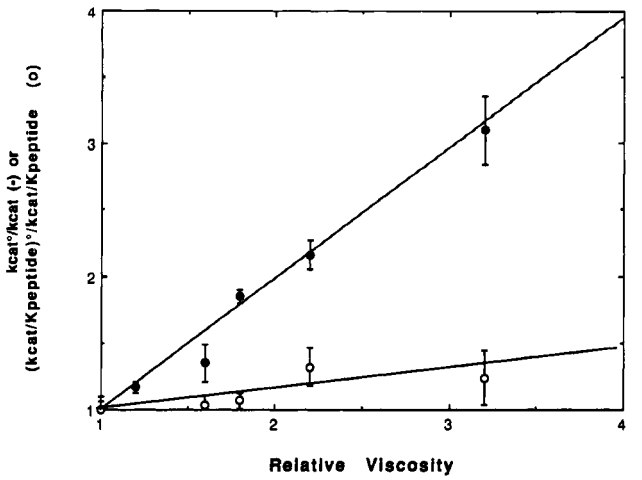

FIGURE 2: Dependence of the steady-state kinetic parameters for peptide I on the relative viscosity of the solution, 100 mM Tris (pH 8.0), 24 °C. η^{rel} is the ratio of the solution viscosity in the presence and absence of viscosogen (glycerol and sucrose; see Materials and Methods). k_{cat}^0/k_{cat} (●) and $(k_{cat}/K_{peptide})^0/k_{cat}/K_{peptide}$ (○) are the ratios of the observed k_{cat} and $k_{cat}/K_{peptide}$ values in the absence and presence of viscosogen, respectively.

Table III: Steady-State Kinetic Parameters and Viscosity Effects for Peptide I at Varied ATP and Fixed Substrate Concentrations[a]

[I] (μM)	$^{app}k_{cat}$ (s^{-1})	K_{ATP} (μM)	$^{app}k_{cat}/K_{ATP}$ (μM^{-1} s^{-1})	$(^{app}k_{cat})^{\eta}$	$(^{app}k_{cat}/K_{ATP})^{\eta}$
50[b]	7.7 ± 0.37	18 ± 3.1	0.42 ± 0.045	0.46 ± 0.10	1.0 ± 0.15
[I] (μM)	$^{*}k_{cat}$ (s^{-1})	K_{ATP} (μM)	$^{*}k_{cat}/K_{ATP}$ (μM^{-1} s^{-1})	$(^{*}k_{cat})^{\eta}$	$(^{*}k_{cat}/K_{ATP})^{\eta}$
2500[c]	8.3 ± 0.10	18 ± 0.24	0.46 ± 0.010	0.38 ± 0.14	0.72 ± 0.16

[a] [ATP] = 10–150 μM, 10 mM free Mg^{2+}, 100 mM Tris (pH 8), and 24 °C. [b] All steady-state kinetic data for nonsaturating kemptide concentrations are expressed with the superscript prefix "app" in the text [e.g., $^{app}k_{cat}$ and $(^{app}k_{cat}/K_{ATP})^{\eta}$]. [c] All steady-state kinetic data for saturating peptide I concentrations are expressed with the superscript prefix "*" in the text [e.g., $^{*}k_{cat}$ and $(^{*}k_{cat}/K_{ATP})^{\eta}$].

An illustration of the dependence between η^{rel} and k_{cat} and $k_{cat}/K_{peptide}$ for peptide I is presented in Figure 2. The relative change in the kinetic parameters at any given η^{rel} is expressed as the ratio of the observed parameter in the absence and presence of viscosogen. Linear dependencies were found between k_{cat}^0/k_{cat}, $(k_{cat}/K_{peptide})^0/(k_{cat}/K_{peptide})$, and η^{rel} for all peptides studied. The slopes associated with these plots are compiled in Table II for conditions of saturating ATP and varied substrate concentrations. The effects of viscosity on the steady-state kinetic parameters under conditions of fixed peptide I and varied ATP concentrations are presented in Table III. For all peptides, the slope values lie between 0 and 1.

The diminution in steady-state kinetic parameters by viscosogenic additives through either global structural perturbations or specific active-site interactions was disregarded for four reasons. First, the enzyme can be dialyzed overnight in buffers containing 36% glycerol and still retain full activity upon dilution. Second, the circular dichroism spectra in the absence and presence of 36% glycerol are indistinguishable, suggesting similar secondary structure conformation (data not shown). Third, viscosogenic effects on $k_{cat}/K_{peptide}$ for good substrates are abolished for poor substrates (Table II). This point was used previously as a general control for viscosogenic inhibitory effects in chymotrypsin (Brower & Kirsch, 1982). Fourth, the intrinsic ATPase rate of the catalytic subunit is unaffected by viscosogenic agents. Since the enzyme-mediated transfer of the γ phosphate of ATP to water is catalyzed at a rate constant that is some 1300-fold slower than that of the peptide I reaction, the rate-determining step for ATPase activity is nondiffusive (Cook et al., 1982). A catalytic subunit concentration of 6.4 μM converted 4.3 and 4.0 μM of ATP to ADP per minute in 0 and 30% sucrose-containing buffers, respectively, at 1 mM ATP and 10 mM free Mg^{2+}.

DISCUSSION

Despite the considerable work done on the kinetic mechanism of cAPK (Whitehouse et al., 1983; Cook et al., 1982; Yoon & Cook, 1987), no direct experimental observations have put kinetic limits on the chemical and product release steps. The evidence for rate-determining chemistry or product release is, to date, conflicting. Cook et al. (1982) asserted that since the K_m for peptide I is more than 10-fold lower than its K_d value, a rapid transformation, namely, peptide phosphorylation, occurs directly after the formation of the central substrate complex E·ATP·S, leaving ADP desorption as the rate-determining step under V_{max} conditions. However, a rapid conformational change followed by slower chemistry cannot be eliminated. Metal dependencies on V_{max} for the intrinsic ATPase activity of cAPK led Armstrong et al. (1979) to conclude that phosphotransfer limits V_{max}. This conclusion follows from the equivalent effects of metal substitution on the ATPase and peptide I reaction rates, although compensatory effects on phosphorylation and product dissociation rates due to metal replacement cannot be disregarded. Comparative studies show that V_{max} is insensitive to changes in the consensus sequence of short peptidic substrates while V_{max}/K_m varies by several orders of magnitude [see review (Järv & Ragnarsson, 1991)]. This implies a common kinetic process at high substrate levels although it does not differentiate between rate-determining chemistry and product release.

Manipulation of solvent viscosity has been used previously to test the diffusion-controlled limits for a number of enzyme-catalyzed reactions. Attenuation of k_{cat}/K_m for *p*-nitrophenyl and methyl ester substrates of chymotrypsin shows that the rates of acylation occur at 40% and 10% of the diffusion-controlled limits, respectively (Brower & Kirsch, 1982). Viscosity studies of the hydrolysis of substrates by the phosphotriesterase of *Pseudomonas diminuta* lead to the proposal of a kinetic mechanism limited by chemical transformation and product dissociation for highly acidic and basic leaving groups of the substrate, respectively (Caldwell et al., 1991). With these and other studies as precedents (Blacklow et al., 1988; Stone & Morrison, 1988), we measured the effects of solvent viscosity on the phosphorylation reactions catalyzed by cAPK using four synthetic peptides (Table I). These peptides were selected on the basis of their wide specificity range for the active site of cAPK (Table II). The results test the role of substrate and product diffusion on the steady-state kinetic parameters.

The encounter rate for two molecules in solution is indirectly proportional to the viscosity of the solvent medium at a given temperature (Caldin, 1964). For a simple bimolecular process as described in eq 2, the rate constants k_1 and k_{-1}, the diffusion-

$$A + B \underset{k_{-1}}{\overset{k_1}{\rightleftharpoons}} AB \qquad (2)$$

controlled rate constants for association and dissociation, respectively, are inversely related to the intrinsic viscosity of the solution. The relative solution viscosity (η^{rel}) can then be

Table IV: Estimates of the Microscopic Rate Constants for Scheme III from Viscosity Measurements

parameter	I (kemptide)	II (chocktide)	III
$k_1°$ [a] (μM^{-1} s^{-1})	0.4 ± 0.1		
$k_{-1}°$ [b] (s^{-1})	≤6		
$k_2°$ [c] (μM^{-1} s^{-1})	3 ± 2	1.4 ± 0.4	1.0 ± 0.3
$k_{-2}°$ [d] (s^{-1})	≥800	≥130	≥140
k_3[e] (s^{-1})	≥210	≥80	≥180
$k_4°$ [e] (s^{-1})	22 ± 1	20 ± 2	20 ± 2
$*k_1$[f] (μM^{-1} s^{-1})	0.64 ± 0.18		
$*k_{-1}$[g] (s^{-1})	≤7		
k_c[h] (s^{-1})	14 ± 8		
k_3/k_{-2}[i]	0.15 ± 0.09	0.67 ± 0.22	0.82 ± 0.36

[a] $k_1°$ is derived from eqs 9 and 11 and ${}^{app}k_{cat}/K_{ATP}$ and $({}^{app}k_{cat}/K_{ATP})^{\eta}$ (Table III). [b] $k_{-1}°$ is derived from eq 9, $k_1°$, $k_2°$, $k_{-2}°$, and k_3. [c] $k_2°$ is derived from eq 5 and k_3/k_2. [d] $k_{-2}°$ is derived from eq 7, k_3, and $k_{cat}/K_{peptide}$ (Table II). [e] k_3 and k_4 are derived from eq 6 and k_{cat} and $(k_{cat})^{\eta}$ (Table I). [f] $*k_1$ is derived from eqs 13 and 15 and $*k_{cat}/K_{ATP}$ and $(*k_{cat}/K_{ATP})^{\eta}$ (Table III). [g] $*k_{-1}$ is derived from eq 15 and k_c. [h] k_c is derived from eq 14, $k_4°$, and $(*k_{cat})^{\eta}$ (Table III). [i] k_3/k_{-2} is derived from eq 7 and $(k_{cat}/K_{ATP})^{\eta}$ (Table II).

Scheme I

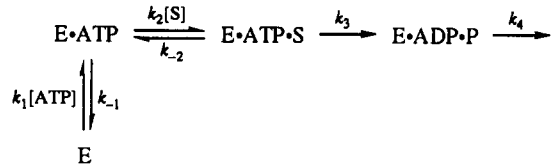

equated to the ratio of the microscopic rate constants in eq 2 according to eq 3, where η^{rel} is the ratio of the solution

$$k^0_1/k_1 = k^0_{-1}/k_{-1} = \eta^{rel} \quad (3)$$

viscosity in the presence and absence of viscosogen and k^0_1 (k^0_{-1}) and k_1 (k_{-1}) are the rate constants in the absence and presence of viscosogen, respectively.

Interpretation of Viscosity Data: (*A*) *Saturating ATP and Varying Peptide Concentrations*. Scheme I satisfies the minimal kinetic requirements for peptide phosphorylation by cAPK under conditions of saturating ATP concentration. In this mechanism the substrate combines with the E•ATP complex to form the active central complex, E•ATP•S, by the second-order association rate constant, k_2, and the dissociation rate constant, k_{-2}. The catalytic step, k_3, is the unimolecular rate constant that describes the chemical transfer of the γ phosphate of ATP to the hydroxyl functional group of the peptide as well as any viscosity-independent conformational changes associated with this transfer. This step is assumed to be energetically favorable since k_{cat} for the reverse reaction catalyzed by the catalytic subunit (i.e., peptide dephosphorylation) is 250-fold slower than the maximal rate in the forward reaction (Cook et al., 1982). The irreversibility of the phosphorylation step was also found for the reaction catalyzed by type II calmodulin-dependent protein kinase (Caldwell et al., 1991). For this enzyme the reverse reaction is ~800-fold slower than the forward k_{cat}. Finally, the dissociation of products, ADP and phosphorylated peptide, is combined in k_4. Owing to the reduced affinity of the phosphorylated peptide I (K_d > 1 mM; Whitehouse et al., 1983) compared to ADP (K_i = 10 μM; Cook et al., 1982), the rate-determining step for product dissociation is ADP release. Thus, k_4 will refer to the dissociation rate constant of ADP alone. Although product dissociation is written as a single unimolecular step, there may be a number of conformational changes associated with the release of ADP. It is possible that these changes are sensitive to viscosity, particularly if they involve large movements of protein structure. These mechanistic fine points cannot be unequivocally partitioned with these techniques.

By using Cleland's method of net rate constants (Cleland, 1975), rate equations for k_{cat} and $k_{cat}/K_{peptide}$ can be derived. Equations 4 and 5 relate the microscopic rate constants of

$$k_{cat} = k_3k_4/(k_3 + k_4) \quad (4)$$

$$k_{cat}/K_{peptide} = k_2k_3/(k_{-2} + k_3) \quad (5)$$

Scheme I to the steady-state kinetic parameters. Since k_2, k_{-2}, and k_4 are presumed to represent diffusion-controlled processes, these rate constants will be dependent on the relative viscosity of the solvent. By taking separately the ratio of eqs 4 and 5 in the absence and presence of viscosogen according to eq 3, two linear equations are derived upon plotting $k_{cat}{}^0/k_{cat}$ and $(k_{cat}/K_{peptide})^0/(k_{cat}/K_{peptide})$ as a function of η^{rel}. The slopes of these lines are given by

$$(k_{cat})^{\eta} = k_3/(k_3 + k_4{}^0) \quad (6)$$

and

$$(k_{cat}/K_{peptide})^{\eta} = k_3/(k_{-2}{}^0 + k_3) \quad (7)$$

where $k_{-2}{}^0$ and $k_4{}^0$ are the dissociation rate constants of substrate peptide and ADP, respectively, when $\eta^{rel} = 1$. Thus, $(k_{cat})^{\eta}$ and $(k_{cat}/K_{peptide})^{\eta}$ can vary between 0 and 1, the diffusion-controlled limit. When the chemical step is much faster than ADP release (i.e., $k_3 \gg k_4{}^0$), $(k_{cat})^{\eta}$ approaches the limiting value of 1. Likewise, when the substrate is sticky (i.e., $k_3 \gg k_{-2}{}^0$), $(k_{cat}/K_m)^{\eta}$ approaches the limit of 1. For these latter conditions, $k_{cat}/K_{peptide}$ is the association rate constant for E and S, $k_2{}^0$.

For all peptides studied, $(k_{cat})^{\eta} \cong 1$ when the concentration of ATP is high. Thus, the chemical step must be sufficiently faster than the rate of ADP dissociation. Since $k_4{}^0 \ll k_3$, only lower limits can be placed on the phosphorylation step given the error limits associated with the slope measurements (Table II). The calculated values for $k_4{}^0$ and k_3 for three of the four peptides are presented in Table IV. The values of $(k_{cat}/K_{peptide})^{\eta}$ lie between the values of 0 for peptide IV and 0.45 for peptide III. For peptide IV, the rate constant for substrate dissociation far exceeds the rate constant for phosphorylation ($k_{-2}{}^0 \gg k_3$). The rapid equilibrium binding of this substrate results in a $k_{cat}/K_{peptide}$ value far below the expected 10^7–10^8 M^{-1} s^{-1} for a diffusion-controlled reaction (Hammes & Schimmel, 1970). As substrate binding affinity increases for peptides I, II, and III, the slopes increase, indicating a shift from rapid equilibrium binding for the poorest substrate to more catalytically committed substrates (i.e., $k_{-2}{}^0 \approx k_3$). Due to the lower limit established for k_3, only lower limits can be placed on the dissociation rate constants for these peptides (Table IV). For peptides I–III, catalytic commitment factors (k_3/k_{-2}) are modest and lie within the range of 0.2–0.8 (Table IV). The association rate constants for the peptides ($k_2{}^0$) can then be estimated from these factors according to eq 5.

(*B*) *Low Peptide I and Varied ATP Concentrations*. Scheme I is also capable of predicting the viscosity effects on the steady-state kinetic parameters for conditions of low peptide I (50 μM) and varied ATP. The available steady-state kinetic data for cAPK suggests that the preferred binding of ligands is ordered with ATP adding before peptide I (Whitehouse et al., 1983). Although there are dissenting views on this requirement (Cook et al., 1982), at saturating ATP (1 mM) and low peptide I concentrations a random addition can be viewed as

ordered because of the enzyme's higher affinity for ATP compared to that of peptide I. Since $k_3 < k_{-2}$, the binding of the fixed substrate can be treated as a rapid equilibrium step. $^{app}k_{cat}$ and $^{app}k_{cat}/K_{ATP}$ can then be expressed as in

$$^{app}k_{cat} = \frac{k_3k_4[S]/K_s}{[S](k_3 + k_4)/K_s + k_4} \quad (8)$$

and

$$^{app}k_{cat}/K_{ATP} = \frac{k_1k_3[S]/K_s}{k_3[S]/K_s + k_{-1}} \quad (9)$$

where $K_s = k_{-2}/k_2$. Both steady-state kinetic parameters are designated with the superscript/prefix "app" since the substrate concentration is not saturating. The slopes of the plots of the steady-state kinetic parameters vs η^{rel} are expressed in eqs 10 and 11. Equation 10 predicts that the sensitivity of $^{app}k_{cat}$

$$(^{app}k_{cat})^{\eta} = \frac{k_3[S]/K_s}{[S](k_3 + k_4^0)/K_s + k_4^0} \quad (10)$$

$$(^{app}k_{cat}/K_{ATP})^{\eta} = \frac{k_3[S]/K_s}{k_3[S]/K_s + k_{-1}^0} \quad (11)$$

toward the viscosogenic agent declines as [S] is lowered. This was found to be true for low peptide I concentrations [compare $(k_{cat})^{\eta}$ for peptides I–III in Table II to $(^{app}k_{cat})^{\eta}$ for peptide I in Table III at 50 μM]. Since $(^{app}k_{cat}/K_{ATP})^{\eta} = 1$, $k_3[S]/K_s > k_{-1}^0$ and $k_{cat}/K_{ATP} = k_1$ (0.4 μM^{-1} s^{-1}; Table III). An upper limit can then be placed on k_{-1} since $K_s \geq 800$ $s^{-1}/3$ μM^{-1} s^{-1} = 250 μM (Table IV) and $k_3 \geq 210$ s^{-1} (Table IV). Without direct measurements of the K_ds for peptide I and ATP, the viscosity experiments predict values close to those obtained from independent methods in other laboratories. Values of $K_s \geq 250$ μM and $K_d(ATP) \leq 15$ μM compare well with other values of K_d = 180 μM for acetyl-peptide I (Whitehouse et al., 1983) and K_i = 10 μM for ATP (Cook et al., 1982).

(C) Varied ATP and Saturating Concentrations of Peptide I. The simple kinetic mechanism of Scheme I cannot explain fully the viscosity data under conditions of saturating peptide I. When the fixed concentration of peptide I is 50 μM the observed maximal velocity at saturating ATP (Table III) is at a value predicted by simple Michaelis–Menten kinetics [(21 s^{-1})(50 μM)/(50 μM + $K_{peptide}$) = 8.8 s^{-1} vs 7.7 s^{-1}, Table III]. However, $^{app}k_{cat}$ does not increase when the concentration of peptide I is raised from below to 40-fold above the $K_{peptide}$ value (Table III). In plots of observed rate vs peptide I concentration the data deviate from a simple hyperbolic relationship above 250 μM peptide I (Figure 1). This substrate inhibition was observed previously by other workers using radiolabeled ATP and a filter binding assay for phosphorylated peptide I (Whitehouse et al., 1983). These authors concluded that peptide I binds weakly to the catalytic subunit inducing an unproductive binary complex. This complex was shown to be catalytically competent through isotopic partitioning methods (Kong & Cook, 1988). The data in the plot of Figure 1 do not approach zero at high concentrations of peptide I. These data and the data presented in Table III indicate that ATP can bind to the enzyme·peptide complex and undergo catalysis, although at a reduced rate.

Scheme II accommodates the unproductive peptide I complex (*E·S) where K_s is the dissociation constant for peptide I and the free enzyme, $*k_1$ and $*k_{-1}$ are the association and dissociation rate constants for ATP and the unproductive

Scheme II

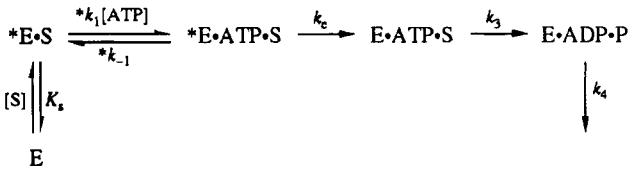

binary complex, respectively, k_c is an irreversible, viscosity-independent step separating the unproductive and productive ternary complexes, and k_3 and k_4 are the same as in Scheme I. Three assumptions are made in this mechanism: first, S binds to the free enzyme and induces an unproductive form, *E·S, which then binds ATP; second, phosphorylation occurs through a unique ternary complex, E·ATP·S; and third, k_c is slow relative to the phosphorylation step (k_3).[2] Since 2500 μM peptide I is capable of trapping 100% of the free enzyme on the basis of the dissociation constant measured by equilibrium dialysis (Whitehouse et al., 1983) and the lower limit set on K_s from viscosity data (Table IV), Scheme II dominates over the kinetic pathway presented in Scheme I. Thus, steady-state rate equations can be written for Scheme II when substrate is saturating since $k_3 > k_c$:

$$*k_{cat} = k_ck_4/(k_c + k_4) \quad (12)$$

$$*k_{cat}/K_{ATP} = *k_1k_c/(*k_{-1} + k_c) \quad (13)$$

where $*k_{cat}$ and $*k_{cat}/K_{ATP}$ are the maximal velocity and second-order rate constant, respectively, for the phosphorylation reaction under conditions of saturating peptide I and varying ATP concentrations. The superscript prefix "*" is used for both steady-state kinetic parameters to distinguish them from the other parameters measured at saturating ATP (i.e., no prefix) and nonsaturating substrate (i.e., "app") conditions. Applying the same viscosity constraints as for eqs 6 and 7, the slopes of the viscosity-dependent steady-state kinetic parameters are

$$(*k_{cat})^{\eta} = k_c/(k_c + k_4^0) \quad (14)$$

and

$$(*k_{cat}/K_{ATP})^{\eta} = k_c/(*k_{-1}^0 + k_c) \quad (15)$$

Unlike the conditions of saturating ATP, $*k_{cat}/K_{ATP}$ is more sensitive to solution viscosity than is $*k_{cat}$ (Table III). The decrease in maximal velocity at high peptide I concentrations (Figure 1) cannot be explained by the substrate decreasing the dissociation rate constant for ADP since this synergistic effect would not change the rate of phosphorylation and the sensitivity of $*k_{cat}$ toward viscosogen. Since $(*k_{cat})^{\eta} = 0.38 \pm 0.14$ and $k_4^0 = 22$ s^{-1} (Table IV), the inductive step, k_c, can be calculated to be 14 ± 8 s^{-1} (Table IV). Unlike the rapid phosphorylation of peptide I at high ATP concentrations, the observed chemical step, k_c, is decreased at high peptide. This effect allows k_c and ADP dissociation (k_4^0) to share in rate limitation. Due to the direct measurement of k_c and $(*k_{cat}/K_{ATP})^{\eta}$, an upper limit of 7 s^{-1} can be placed on the dissociation rate constant, $*k_{-1}^0$, for ATP and *E·S complex. Since ($*k_{cat}$/

[2] This latter assumption derives necessarily from the usage of a common ternary complex. If the productive complex could be converted rapidly to an unproductive complex through an equilibrium step, the observed attenuation in the phosphorylation rate would be equivalent whether ATP or peptide I were saturating. This is not observed. k_c is written as an irreversible step since the phosphorylation step is fast and does not permit the return of E·ATP·S to *E·ATP·S.

Scheme III

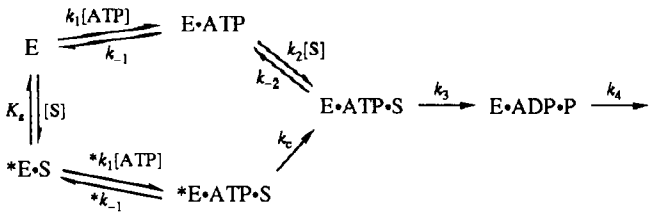

$K_{ATP})^{\eta} = 0.72 \pm 0.16$ and $^*k_{cat}/K_{ATP} = 0.46\ \mu M^{-1}\ s^{-1}$, $^*k_1{}^0 = 0.64 \pm 0.18\ \mu M^{-1}\ s^{-1}$ (Tables III and IV). Note that the viscosity data predict that ATP has similar affinity for the free enzyme ($k_{-1}/k_1 \leq 15\ \mu M$) and the unproductive binary complex, *E•S ($^*k_{-1}/^*k_1 \leq 15\ \mu M$).

Complete Kinetic Scheme. The viscosity-dependent steady-state kinetic data can be combined to outline a complete kinetic mechanism for the catalytic subunit of cAPK. Scheme III describes the sequential-step processing of ATP and S under all ligand concentrations. Table IV compiles the rate constants associated with this mechanism that were determined from steady-state kinetic data. Although the mechanism is formally random sequential, there is a preferred binding order under limiting amounts of peptide with ATP binding first. At higher peptide concentrations ATP binds to form an unproductive enzyme/peptide conformer that only slowly delivers phosphate. It is presently not possible to define the structural details of this altered enzyme species. However, the X-ray crystal structure (Knighton et al., 1991) of the binary enzyme/peptide complex of the catalytic subunit indicates that ATP binds deep within the active-site groove with the peptide directly lining the periphery. It is likely that ATP prebinding directs the productive association of substrate. In the presence of a large substrate pool, however, bound peptide I adjusts its conformation upon ATP binding to position the γ phosphate for delivery.

The deduction of the rate constants defining Schemes I and II (Table IV) was performed under extreme concentrations of either ATP or peptide I (i.e., saturating ATP, varying peptide or saturating peptide, varying ATP). The test of the validity of the combined mechanism of Scheme III lies in its ability to predict initial reaction velocities under intermediate nucleotide and substrate concentrations. The kinetic simulation program HopKINSIM[3] was used to predict initial reaction velocities for Scheme III under the kinetic constraints listed in Table IV. Table V lists both the experimental and calculated values for v^0/E_t over a wide range of ATP and substrate concentrations. In all simulations, 250 μM was used as the dissociation constant, K_s, for peptide I on the basis of viscosity-dependent estimates (Table IV). It was assumed that the binding of ATP does not affect greatly the affinity of peptide I (i.e., $K_s = k_{-2}/k_2$). Kinetic simulations of the initial reaction velocity for peptide I phosphorylation, were also performed under conditions of fixed ATP. The simulated reaction velocity at 100 μM ATP and varied peptide is presented in Figure 1. The best approximation of the experimental data at both low (inset) and high peptide concentrations was achieved with $k_{-2}/k_2 = 1000\ s^{-1}/2\ \mu M^{-1}\ s^{-1} = 500\ \mu M$. The consistency of calculated and experimental rate parameters at varying ligand concentrations supports the mechanism of Scheme III for the enzyme-catalyzed phosphorylation of peptide I.

[3] HopKINSIM is a kinetic simulation program adapted for the Macintosh computer by Danny Wachsstock at Johns Hopkins University School of Medicine. HopKINSIM is derived from the kinetic simulation program KINSIM (Barshop et al., 1983).

Table V: Experimental and Calculated Initial Velocity Measurements for the cAPK-Catalyzed Phosphorylation of Peptide I under Varying Concentrations of ATP and Kemptide[a]

[ATP][b] (μM)	[peptide I] (μM)	v^0/E_t (s^{-1}) calcd	v^0/E_t (s^{-1}) exptl
17	250	4.2	4.4
20	50	4.4	4.0
20	2500	3.6	4.4
50	150	7.4	8.3
100	150	9.2	10
133	250	9.1	11
133	5000	7.1	7.4
1000	9.1	3.3	2.4
1000	50	9.6	8.7
1000	150	13	14

[a] The calculated values of v^0/E_t were determined by fitting the experimental data of Table IV to Scheme III using the kinetic simulation program HopKINSIM.[3] [b] Free Mg^{2+} concentration is 10 mM.

It was demonstrated through these viscosity experiments that the observed association rate constants for nucleotide and substrate are 1–2 orders of magnitude below the expected diffusion-controlled limit (Hammes & Schimmel, 1970). Estimates of the association rate constants from isotope partitioning experiments also hint toward reduced values (Kong & Cook, 1988). Thus, the binding of these ligands requires additional steps before phosphate acceptor and donor are appropriately positioned. These steps may include solvent reorganization or ligand and protein conformational adjustments. Circular dichroism studies of the catalytic subunit indicate that several discrete structural changes occur during the association of peptide analogs. Reed et al. (1985) concluded that a minimum of three steps are required for substrate docking. These steps involve an increase in β structure and a decrease in α-helical structure. These structural accommodations may be the cause of the large diffusional barrier for substrate binding.

Although it was shown through stereochemical approaches (Ho et al., 1988) that no covalent phosphoryl/enzyme species develops, the data in this manuscript predict that a rapid production of ADP should occur before establishment of steady-state turnover. This is the result of the slow dissociation rate of this ligand compared to the rate of phosphoryl transfer. When the substrate is largely increased relative to the nucleotide concentration, no accumulation of ADP occurs due to the slow step separating unproductive and productive complexes.

ACKNOWLEDGMENT

We thank Drs. Bryan Driscoll and Patricia Jennings for critical reading of the manuscript and many helpful discussions. We also thank Siv Garrod for the HPLC purification of the peptides and Karen Prather for the purification of the catalytic subunit.

REFERENCES

Armstrong, R. N., Kondo, H., & Kaiser, E. T. (1979) *Proc. Natl. Acad. Sci. U.S.A. 76*, 722.

Barshop, B. A., Wrenn, R. F., & Frieden, C. (1983) *Anal. Biochem. 130*, 134–145.

Blacklow, S. C., Raines, R. T., Lim, W. A., Zamore, P. D., & Knowles, J. R. (1988) *Biochemistry 27*, 1158–1167.

Brower, A. C., & Kirsch, J. F. (1982) *Biochemistry 21*, 1302–1307.

Caldin, E. F. (1964) *Fast Reactions in Solution*, pp 10–11, Wiley, New York.

Caldwell, S. R., Newcomb, J. R., Schlecht, K. A., & Rauschel, F. M. (1982) *Biochemistry 30*, 7438–7444.
Cleland, W. W. (1975) *Biochemistry 14*, 3220–3224.
Cook, P. F., Neville, M. E., Jr., Vrana, K. E., Hartl, F. T., & Roskoski, R., Jr. (1982) *Biochemistry 21*, 5794–5799.
Cooper, J. A. (1990) in *Peptides and Protein Phosphorylation* (Kemp, B. E., Ed.) pp 85–114, CRC Press, Inc., Boca Raton, FL.
Feramisco, J. R., & Krebs, E. G. (1978) *J. Biol. Chem. 253*, 8968.
Granot, J., Mildvan, A. S., Bramson, H. N., Thomas, N., & Kaiser, E. T. (1981) *Biochemistry 20*, 602–610.
Hammes, G. G., & Schimmel, P. R. (1970) *Enzymes (3rd Ed.) 2*, 67–114.
Hanks, S. K., Quinn, A. M., & Hunter, T. (1988) *Science 241*, 42–52.
Ho, M.-f., Bramson, H. N., Hansen, D. E., Knowles, J. R., & Kaiser, E. T. (1988) *J. Am. Chem. Soc. 110*, 2686–2681.
Hunter, T., & Cooper, J. A. (1986) *Enzymes (3rd Ed.) 17*, 92–113.
Järv, J., & Ragnarsson, U. (1991) *Bioorg. Chem. 19*, 77–87.
Kemp, B. E., Bylund, D. B., Huang, T. S., and Krebs, E. G. (1975) *Proc. Natl. Acad. Sci. U.S.A. 72*, 3448–3452.
Kemp, B. E., Graves, D. J., Benjamini, E., & Krebs, E. G. (1977) *J. Biol. Chem. 252*, 4888.
Knighton, D. R., Zheng, J., Ten Eyck, L. F., Ashford, V. A., Xuong, N.-h., Taylor, S. S., & Sowadski, J. M. (1991a) *Science 253*, 407–413.
Knighton, D. R., Zheng, J., Ten Eyck, V. A., Xuong, N.-h., Taylor, S. S., & Sowadski, J. M. (1991b) *Science 253*, 414–420.
Kong, C.-T., & Cook, P. F. (1988) *Biochemistry 27*, 4795–4799.
Reed, J., Kinzel, V., Kemp, B. E., Cheung, H.-C., & Walsh, D. A. (1985) *Biochemistry 24*, 2967–2973.
Shoemaker, D. P., & Garland, C. W. (1962) *Experiments in Physical Chemistry*, 2nd ed., McGraw-Hill, New York.
Slice, L. C., & Taylor, S. S. (1989) *J. Biol. Chem. 264*, 20940–20946.
Stone, S. R., & Morrison, J. F. (1982) *Biochemistry 27*, 5493–5499.
Taylor, S. S., Buechler, J. A., & Yonemoto, W. (1990) *Annu. Rev. Biochem. 59*, 971–1005.
Walsh, D. A., Perkins, J. P., & Krebs, E. G. (1968) *J. Biol. Chem. 243*, 3763.
Whitehouse, S., Feramisco, J. R., Casnellie, J. E., Krebs, E. G., & Walsh, D. A. (1983) *J. Biol. Chem. 258*, 3693–3701.
Wright, D. E., Noiman, E. S., Chock, P. B., and Chau, V. (1981) *Proc. Natl. Acad. Sci. U.S.A. 73*, 6048–6050.
Yonemoto, W. M., McGlone, M. L., Slice, L. W., & Taylor, S. S. (1991) *Methods Enzymol. 200*, 581–596.
Yoon, M.-y., & Cook, P. F. (1987) *Biochemistry 26*, 4118–4125.